

RESEARCH ARTICLE

Evaluation of circulation-type classifications with respect to temperature and precipitation variations in the central and eastern Tibetan Plateau

Xiaowen Zhang^{1,2}  | Deliang Chen^{3,4}  | Tandong Yao^{1,4}

¹Key Laboratory of Tibetan Environment Changes and Land Surface Processes, Institute of Tibetan Plateau Research, Chinese Academy of Sciences, Beijing, China

²University of Chinese Academy of Sciences, Beijing, China

³Regional Climate Group, Department of Earth Sciences, University of Gothenburg, Gothenburg, Sweden

⁴CAS Center for Excellence in Tibetan Plateau Earth Sciences, Chinese Academy of Sciences, Beijing, China

Correspondence

Xiaowen Zhang, Key Laboratory of Tibetan Environment Changes and Land Surface Processes, Institute of Tibetan Plateau Research, Chinese Academy of Sciences, Beijing 100101, China.

Email: zhangxw@itpcas.ac.cn

Funding information

National Natural Science Foundation of China, Grant/Award Number: 91537210; the Strategic Priority Research Program of Chinese Academy of Sciences (XDA20060401); Swedish Foundation for International Cooperation in Research and Higher Education.

Circulation-type classifications (CTCs) are useful tools for systematically describing atmospheric circulation and studying its variation and impact on surface climate. However, few circulation classification methods (CCMs) have been applied in the Tibetan Plateau (TP). In this study, six frequently used CCMs using 500 hPa geopotential height data were assessed with respect to their abilities in explaining observed daily mean temperature and precipitation variations in the central and eastern TP for the period 1980–2014. Two statistical measures, the explained variance and the Kolmogorov–Smirnov test, were used to quantify the performance of the CTCs in describing climate variable variations. SAN (simulated annealing and diversified randomization clustering) and KRZ (Kruizinga's eigenvector-based scheme) were identified as optimum CCMs for synoptic typing over the study region. The daily mean temperatures are well conditioned on SAN-CTC with 43.9–62.4% explained variance at annual scale and 11.1–25.2% at seasonal scale. For daily precipitation variations, the explained variance at the annual scale is less than 40%. The spatial characters of climate variation affected by large-scale circulation are identified. Daily mean temperature variations in the Qaidam Basin and the Qilian Mountains (90°–103°E and 35°–40°N) all year round and in the region between the Tanggula Mountains and the Himalayan Mountains (88°–97°E and 30°–34°N) in wet season (May–September) are well resolved by the CTCs. Daily precipitation variations in the eastern TP in the dry season (October–April) and a region from the Brahmaputra River basin to the Tanggula Mountains (85°–92°E and 28°–32°N) and the southern Hengduan Mountains (98°–102°E and 27°–31°N) in the wet season show a close relationship with the identified CTCs by SAN.

KEYWORDS

circulation classification, COST733, precipitation, synoptic climatology, temperature, Tibetan Plateau

1 | INTRODUCTION

The Tibetan Plateau (TP) is a large area of high elevation that has a profound influence on atmospheric circulation over Asia and beyond via mechanical and thermal dynamical effects (Ye and Gao, 1979; Ye and Wu, 1998; Wu *et al.*, 2015). The TP acts as an important modulator of regional

climate over central and southern Asia and creates a unique plateau climate. In recent decades, ample evidence has revealed that the TP has undergone faster warming than the global average and other areas with similar latitudes (Liu and Chen, 2000; Chen *et al.*, 2015)

Regional climate variations can be caused by large-scale atmospheric circulation variations. Therefore, investigations

concerning climate variations should not only be restricted to climate variables, such as temperature and precipitation, but also include atmospheric circulation dynamics. Hence, it is necessary to explore the long-term trends and variability in large-scale circulation as well as the links between circulation and climate variability at different temporal and spatial scales (Corte-Real *et al.*, 1998; Kyselý, 2002). Studying the variation of atmospheric circulation depends on the availability of an effective method to capture the typical circulation patterns/circulation types (CTs, usually a centroid of a group of similar circulation patterns) in an immense and boundless continuum of individual instantaneous circulation patterns.

In the past decades, a number of circulation classification methods (CCMs) have been proposed and used. Huth *et al.* (2008) characterized the varied methodologies and approaches of circulation classification into three basic groups: subjective (manual), hybrid (usually refers to a computer-assisted version of subjective methods) and objective (automated). In subjective CCMs, CTs are usually identified by experienced meteorologists based on their expert knowledge (Baur *et al.*, 1944; Hess and Brezowsky, 1952) or physical/geometrical considerations (e.g., Lamb, 1950; 1972), and circulation patterns are then classified by visual inspection in a manual process. This kind of methods suffers from considerable limitations, such as subjectivity, non-portability, non-repeatability and extremely high time consumption. With the advancement of computers, certain subjective methods have been improved and revised to become hybrid methods in which CTs are subjectively defined a priori and circulation patterns are assigned by similarity measures with computer-assisted processes (Jenkinson and Collison, 1977; Chen, 2000; Jones and Davis, 2000; James, 2006; Beck *et al.*, 2007). In objective methods, a classification procedure is developed based on statistical theory, and only a small number of subjective decisions are involved. Although the definition of the number of CTs remains a task that requires certain subjective decisions, objective methods have been widely used in meteorology and climatology (e.g., Schmutz and Wanner, 1998; Liu *et al.*, 2015; Cahynová and Huth, 2016).

For historical reasons, most classification methods were developed and applied in Europe (e.g., Plaut and Simonnet, 2001; Cahynova and Huth, 2010) and North America (e.g., Cavazos, 1999; Gevorgyan, 2013). Up to now, few studies on circulation classification have been performed in Asia (e.g., Zhu *et al.*, 2007), especially in the TP (Liu *et al.*, 2015). Previous studies have shown that an overall best CCM for all regions or climate variables is not available. The performance of CCMs varies for different spatial domains, periods and variables of focus (Beck and Philipp, 2010). In order to further study the relationship between atmospheric circulation and surface climate on the TP, this study focuses on an evaluation and comparison of several

commonly used CCMs in terms of their ability in explaining the surface air temperature and precipitation over the central and eastern Tibetan Plateau (CETP).

In this paper, an effective and suitable CCM for surface air temperature and precipitation over the CETP is identified in the following manner. The CCMs employed in the comparison, the circulation data, observations and the evaluation measures are described in section 2. A comparison of several CCMs is presented in section 3. A fair comparison of different configurations of CCMs is provided in section 4 at a seasonal scale and is based on a ranking method applied to each of the meteorological stations in the CETP. In section 5, a suitability assessment of CTCs to resolve spatiotemporal climate variations is presented through a further analysis on the ability of CTCs to describe temporal variations of the surface climate variables and their spatial difference.

2 | EVALUATION DATA AND METHODS

2.1 | Circulation classification methods

A program entitled “Harmonisation and Applications of Weather Types Classifications for European Regions” (COST733) was launched in Europe several years ago to assess different methodologies for circulation classifications and analyse the strengths and weaknesses of CCMs for different applications. In COST733, 24 CCMs were divided into six groups based on the basic features of the classification algorithm: threshold-based algorithms, eigenvector-based methods, leader algorithms, hierarchical cluster analysis, optimization algorithms and random classification methods. The CCMs have been evaluated over Europe (Philipp *et al.*, 2014; Huth *et al.*, 2016). Actually, the threshold-based algorithms belong to the hybrid methods, and the other five groups belong to the objective methods.

The cost733class—classification software (Philipp *et al.*, 2016)—is used in this study. However, four kinds of CCMs included in COST733 were omitted from further consideration: (a) CCMs based on multilevel circulation fields, multi-variable or specific variables; (b) hybrid methods, because most were originally designed for a specific region at a specific level; (c) *k*-mean clustering methods that were trapped in local optima and (d) random classification methods because they require large computational resources and are associated with large uncertainties. Therefore, only six CCMs entered the “competition.” A brief summary of the methods that were compared and evaluated in this study is shown in Table 1 along with their abbreviations and brief descriptions.

Because of the high orography of the TP, the mean sea level pressure (SLP) is not a suitable field to find the prevailing circulation patterns over the TP. Moreover, the mean elevation of the TP area in this study is above 4,500 m and 500 hPa level is just above the surface of the TP. Therefore,

TABLE 1 Detail of the circulation classifications compared in this study

Family	Name	Abbreviation	Number of types	Key reference
PCA-based method	Kruizinga	KRZ	9, 18, 27	Kruizinga (1979) and Buishand and Brandsma (1997)
	PCA obliquely rotated	PCT	9, 18, 27	Richman (1986) and Huth (2000)
Leader algorithm	Kirchhofer (sums-of-squares)	KIR	9, 18, 27	Kirchhofer (1974)
	Erpicum and Fettweis	ERP	9, 18, 27	Fettweis <i>et al.</i> (2010)
Optimization method	Simulated annealing and diversified randomization clustering	SAN	9, 18, 27	Philipp <i>et al.</i> (2007)
	Self-organizing maps	SOM	9, 18, 27	Kohonen (1990) and Michaelides <i>et al.</i> (2007)

500 hPa geopotential height field is employed instead of SLP for the classification in this study. The input data used in the classifications were daily mean 500 hPa geopotential height data calculated from the 6-hourly ERA-Interim reanalysis dataset that covered the period from 1980 to 2014 at a $1 \times 1^\circ$ grid resolution, and the dataset was provided by the European Centre for Medium-Range Weather Forecasts (Dee *et al.*, 2011). Four domains with different sizes centered on the TP were selected to represent circulation over the TP. The largest domain (domain 1) covers much of Asia and parts of Europe and Africa, and encompasses most circulation systems known to be relevant to the TP climate variation. The formation and active area of the main influential circulation systems at 500 hPa and an important lower troposphere system is displayed in a schematic diagram (Figure 1). In mid–high latitudes, western disturbances originate in the western Europe and pass across the Mediterranean and the Black and Caspian seas. Another system is a transient wave train that begins in northern Europe and passes over the East European Plain. Furthermore, there are

well-known polar vortex and East Asia trough. In low latitudes, the Iranian high, the monsoon trough, the southwest vortex and the western Pacific subtropical high and the only lower troposphere system “the low-level jet” (Ahasan *et al.*, 2014) all have consequences for surface climate over the TP. The boundaries of the other domains are indented by 10° one by one. Domain 4 is the smallest domain, and it appears like a box frame for the TP. Previous analyses have suggested that the quality of classifications is sensitive to the number of CTs (Huth, 2010; Schiemann and Frei, 2010). To facilitate a fair comparison among the different methods and reduce the influence of quality on the classification, the numbers of CTs were set to 9, 18 and 27 because certain CCMs have restricted the number of CTs based on the concept or constrained by technical reasons.

2.2 | Observed surface climate data

One of the goals of circulation classifications is to aid in understanding the influences of atmospheric circulation on surface climate, which is considered as the main task of synoptic climatology (e.g., Yarnal, 1993; Yarnal *et al.*, 2001). Therefore, whether CTCs can describe variations in surface climate variables, such as surface air temperature and precipitation, and the extent of their explanatory power must be evaluated. Observational records of the daily mean temperature and daily precipitation amount for the period 1980–2014 are used in this study. They are provided by the China Meteorological Data Sharing Service System (<http://data.cma.cn>). There are 112 stations in the TP area in this dataset and the TP area is referred to the plateau extending over 25° – 40° N and 70° – 105° E, with a boundary roughly defined with the elevation above 2,500 m in this paper. As the starts of operations for different stations differ, there are only 80 stations covering the common period during 1980 and 2014. They are mainly situated in the CETP (Figure 2) and are used for the following analysis.

Buishand and Brandsma (1997) have done a comparison of circulation classification schemes for predicting temperature and precipitation in the Netherlands. They found that for daily precipitation characteristics, the classification schemes performed a somewhat higher skill for precipitation occurrence than the daily amount. Therefore, we used occurrence of different magnitude of daily precipitation as an indicator, instead of daily precipitation amount in the following

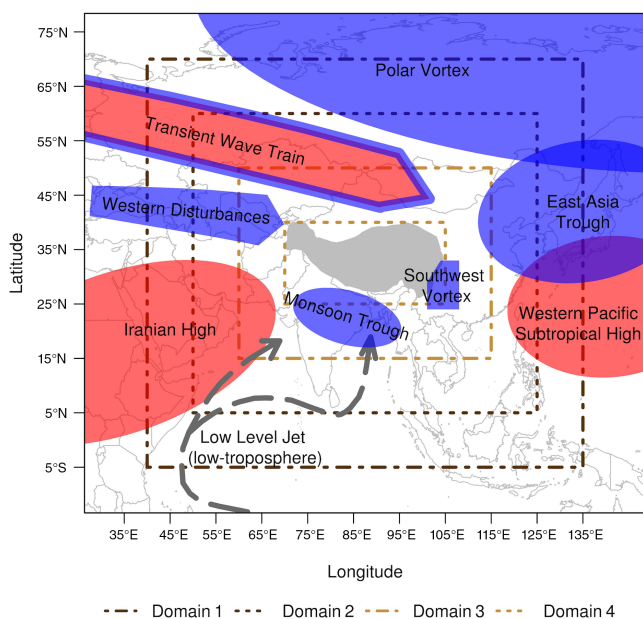


FIGURE 1 Schematic diagram of the circulation systems related to TP climate variations. The boundaries of the four spatial domains for circulation classification are drawn with different kind of dash lines (domain 1: 40° – 135° E, 5° S– 70° N, domain 2: 50° – 125° E, 5° – 60° N, domain 3: 60° – 115° E, 15° – 50° N, domain 4: 70° – 105° E, 25° – 40° N) [Colour figure can be viewed at wileyonlinelibrary.com]

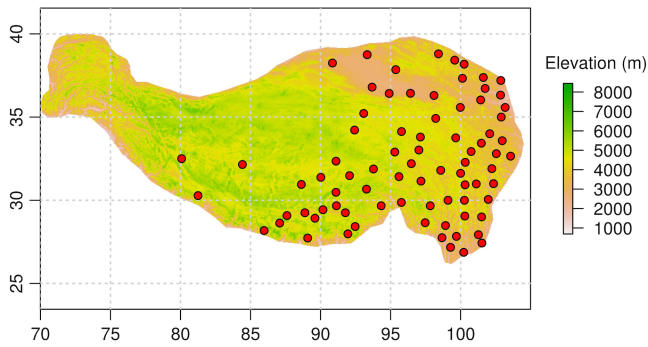


FIGURE 2 Topography of the TP; dots denote the position of the 80 meteorological stations on the TP with continuous record of daily mean temperature and precipitation amount [Colour figure can be viewed at wileyonlinelibrary.com]

analysis. The China Meteorological Administration (CMA) developed a standard to categorize daily precipitation (P) into five intensity groups, when there is a precipitation. We adopted this definition and used numbers 0–5 to represent precipitation categories: 0 means $P < 0.1$ mm/day; 1 means $0.1 \leq P < 10$ mm/day; 2 means $10 \leq P < 25$ mm/day; 3 means $25 \leq P < 50$ mm/day; 4 means $50 \leq P < 100$ mm/day; 5 means $P \geq 100$ mm/day.

2.3 | Evaluation measures

Although an “absolutely correct” CTC is not available, we may flag individual CTCs as more or less suited for particular purposes or possibly even “better” or “worse” than other CTCs; thus, measures of the quality or the application specificity of the CTCs are required. In this study, two measures were used to evaluate the proficiency of CTCs in disaggregating daily mean temperature and precipitation variations via their stratifying ability to group daily values of the climate variables referred to CTC series. Evaluation measures mainly assess two key attributes of the grouped observational data: within-group similarity and between-group separability.

The explained variance (EV) is used to quantify the proportion of the variance present in the dependent variable, which can be accounted for by group membership (Buishand and Brandsma, 1997; Casado *et al.*, 2010; Broderick and Fealy, 2015), and it represents the within-group similarity. The EV is estimated by comparing the within-type variance (within-type sum of squares [WSS]) to the total variance (total sum of squares [TSS]) of the dependent variable and can be written as follows:

$$EV = 1 - \frac{WSS}{TSS}.$$

This statistical value is in the range of 0 to 1, with a value closer to 1 indicating that a CTC possesses the greatest possible explanatory power on the dependent variable.

The second performance measure is calculated based on the two-sample Kolmogorov–Smirnov (KS) test (Tveito,

2010; Broderick and Fealy, 2015). The KS test is a nonparametric test of the equality of continuous one-dimensional probability distributions, and it can be used to compare two samples because it is sensitive to differences in both the location and shape of the empirical cumulative distribution functions of the two samples. Huth (2010) demonstrated that regions that accept or reject the KS test for individual CTCs are geographically coherent, which indicates that the results reflect the physical and meteorological properties of the CTCs. The KS test mainly quantifies the between-group separability, and it is used to perform a comparison between the associated dependent variable distribution functions of each CTC for a given CTC. In this study, once the observed data were grouped according to the CTC, each CTC-specific climate element group was compared using the KS test at the 5% significance level. The rejection of the KS test indicates that the climate variable under the CTC was well separated from the other groups, whereas the acceptance of the KS test implies that the climate variable under the CTC did not significantly differ from the other groups. In this study, the second evaluation measure, KS score, was a ratio of real rejections to all possible rejections of a CTC. To avoid the errors due to small sample size in evaluation procedure, CTCs with a sample size of less than 30 were omitted in both evaluation measures.

3 | COMPARISON OF CCMS

A total of 72 CTCs were obtained, because each CCM had 12 configurations based on different combinations of the four domains and three expected numbers of CTCs. All 72 CTCs were assessed based on their ability to disaggregate the daily mean temperature and precipitation grade of the CETP. The statistical measures outlined above were applied to the 80 station records of the target climate variables. Because of the sensitivity of the statistical measures to the number of CTCs (Broderick and Fealy, 2015; Huth *et al.*, 2016), Figures 3 and 4 show an assessment of the performance of each measure, and target climate variables are coloured according to the expected number of CTCs.

EV is adapted to measure ability of CTCs on capturing the climate element variations and is displayed in the first row in Figures 3 and 4. The KS score represented the separability of the climate variations based on the CTCs series in the view of probability distribution is used as another evaluation criterion and is displayed in the second row in Figures 3 and 4. Furthermore, in order to show the impact of different configurations of the CCMs considered, the results are grouped by the number of CTCs in the left column of figures and in the right column by the size of domain that CCMs were applied on.

The CTCs obtained via SAN (simulated annealing and diversified randomization clustering) performed best and captured approximately 50–60% of the observed variance of

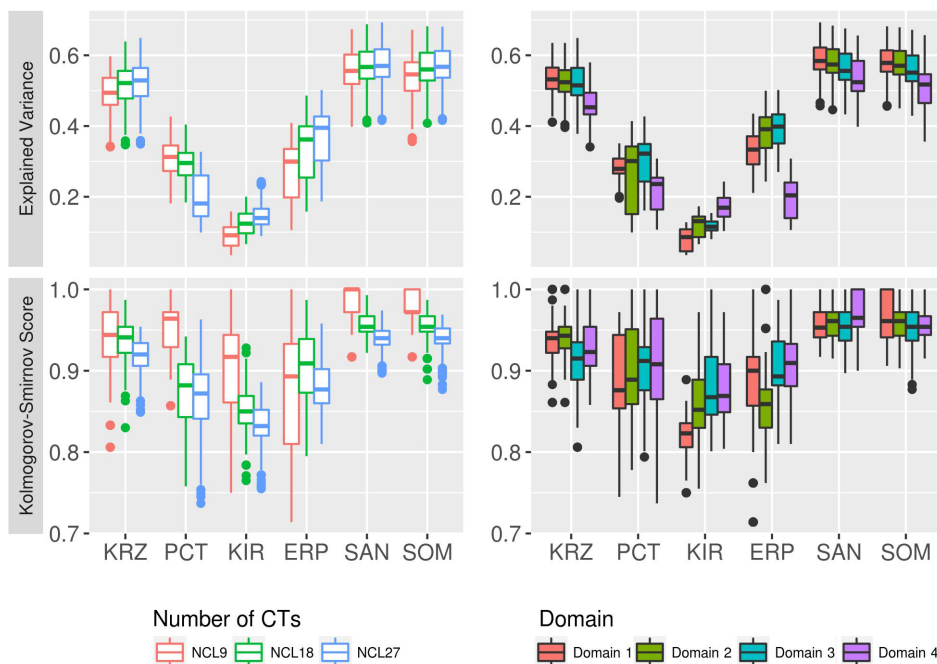


FIGURE 3 EV (top row) and KS score (bottom row) of daily mean temperature calculated based on CTCs obtained from different classification method in 500 hPa. In the left column results of evaluation measures are group by the number of CTs with different colours and in the right column results are group by the size of domain CCMs applied on with different filled colours [Colour figure can be viewed at wileyonlinelibrary.com]

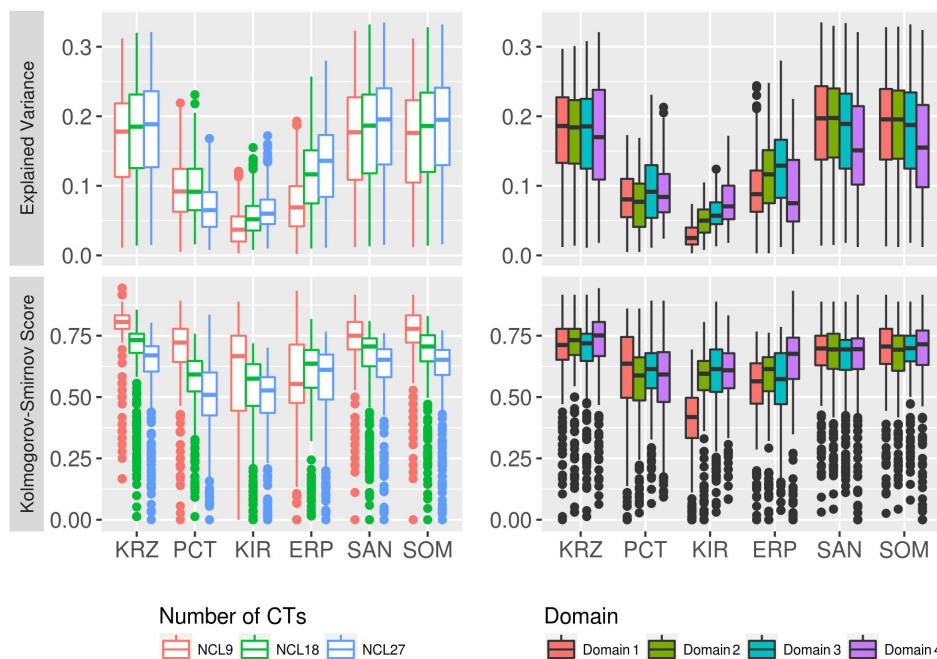


FIGURE 4 EV (top row) and KS score (bottom row) of precipitation grade calculated based on CTCs obtained from different classification method in 500 hPa. In the left column results of evaluation measures are group by the number of CTs with different colours and in the right column results are group by the size of domain CCMs applied on with different filled colours [Colour figure can be viewed at wileyonlinelibrary.com]

daily mean temperature variation, whereas the CTCs obtained by KIR had the worst performance and only captured 15–20% of the observed variance. With respect to the explanatory power of the daily precipitation variations (Figure 4), all CTCs performed poorly and presented EV scores ranging from 0 to 0.33. However, the optimization

methods (SAN and SOM) and KRZ (Kruizinga's eigenvector-based scheme) performed slightly better than the other CCMs. Moreover, boxplots showed that the influence of the configuration on the explanatory power of the CTCs for synoptic-scale variations of the target climate variables was less than the influence of the CCMs.

Compared with the EV performance, the KS scores, which represent between-group separability, exhibited clear dependence on the number of CTs and a slight dependence on the size of the domain. With an increase in the number of CTs, the ability of the CTCs to condition the synoptic-scale variations of the target variables deteriorated. To perform an equitable comparison, the CTCs were assessed on three sub-groups divided by the preset number of CTs, specifically, the 9 CTs sub-group, the 18 CTs sub-group and 27 CTs sub-group. The CTCs of the optimization methods (SAN and SOM) and KRZ were always in the first class for each sub-group and were slightly influenced by the number of CTs. Their KS scores for the daily mean temperature and precipitation grade were approximately 0.95 and 0.75, respectively. These results demonstrate that the CTCs obtained from optimization methods (SAN and SOM) and KRZ do well in conditioning synoptic-scale climate variable variations.

The two statistical measures were used to assess the proficiency of the CTCs in disaggregating the daily mean temperature and precipitation in the CETP from different aspects, and the results suggested that the optimization schemes (SAN and SOM) and KRZ performed better among all the examined CCMs. Their EV scores increased as the number of CTs increased, and their KS scores generally behaved in the opposite manner. The effect of the domain size on the optimization algorithms was small, especially with a larger number of CTs.

4 | RANKING OF CIRCULATION CLASSIFICATION CONFIGURATIONS

Because of the complex terrain of the TP, local effects can be more important in the variation of the climate variables,

TABLE 2 Circulation-type classifications of KRZ ranked (lowest to highest) according to their performance (best to worst) when applied to the daily mean temperature and precipitation for the dry season (October–April) and wet season (May–September). The top one third of CTCs are marked in bold, and the bottom one third of CTCs are marked in italics

CTCs series	Temperature				Precipitation grade			
	Dry season		Wet season		Dry season		Wet season	
	EV	KS	EV	KS	EV	KS	EV	KS
Domain 1_09	<i>10</i>	4	<i>7</i>	<i>12</i>	<i>12</i>	2	<i>12</i>	<i>6</i>
Domain 1_18	<i>5</i>	<i>8</i>	3	<i>10</i>	<i>7</i>	<i>8</i>	<i>10</i>	<i>9</i>
Domain 1_27	1	<i>12</i>	1	<i>7</i>	3	<i>10</i>	<i>7</i>	<i>12</i>
Domain 2_09	<i>8</i>	2	<i>10</i>	3	<i>11</i>	4	<i>11</i>	2
Domain 2_18	<i>6</i>	<i>7</i>	4	1	<i>8</i>	<i>7</i>	<i>6</i>	1
Domain 2_27	2	<i>10</i>	2	2	<i>9</i>	<i>11</i>	2	<i>10</i>
Domain 3_09	<i>7</i>	3	<i>12</i>	<i>11</i>	<i>10</i>	1	<i>9</i>	3
Domain 3_18	4	<i>5</i>	<i>8</i>	<i>6</i>	<i>6</i>	<i>6</i>	<i>5</i>	<i>7</i>
Domain 3_27	3	<i>11</i>	<i>5</i>	<i>8</i>	4	<i>12</i>	3	<i>11</i>
Domain 4_09	<i>12</i>	1	<i>11</i>	4	<i>5</i>	3	<i>8</i>	4
Domain 4_18	<i>11</i>	<i>6</i>	<i>9</i>	<i>5</i>	2	<i>5</i>	3	<i>5</i>
Domain 4_27	<i>9</i>	<i>9</i>	<i>6</i>	<i>9</i>	1	<i>9</i>	1	<i>8</i>

whereas large-scale circulation mainly played a role as a large scale background. Moreover, because of the vast area of the TP, the large-scale circulation influence of the variation of the climate variables differed depending on the location, even with the same CT. For a fair comparison, a ranking of the CTCs was first constructed at each station and then averaged over the 80 stations to obtain integrated rankings under each evaluation measure and for each climate variable.

Additionally, a surface regime specific to a given CT varied depending on season, especially for precipitation. Therefore, separate rankings were conducted for the dry season (October–April) and the wet season (May–September). The definitions of dry season and wet season were based on the typical seasonal variation of the precipitation in the TP (Yao *et al.*, 2013; Gao *et al.*, 2014). According to previous results, the outputs of SOM were almost identical to that of SAN. Therefore, only the CTCs of the KRZ and SAN were ranked in this section for the dry and wet season because SOM is not efficient subjected to its complicated calculations. The top and bottom one third of CTCs were marked in Tables 2 and 3. The performances of statistical measures to assess the within-group similarity and between-group separability were prone to inconsistencies generally. There is no one CTC that ranks high on both evaluation criteria. Nevertheless, by the method of exclusion, certain configurations, such as the configuration of domain 2 with 18 CTs, stands out at explaining climate element variations in the CETP. Although the algorithmic principles of KRZ and SAN are different, similar results of two evaluation measures were obtained, and CTCs in domain 2 with 18 CTs performed better than the other CTCs at resolving the daily mean temperature and precipitation variation for both seasons.

In the typical SAN CTs of 500 hPa geopotential height in domain 2 with 18 CTs (Figure 5), the circulation systems shown in Figure 1 are well displayed except mesoscale structures, such as the southwest vortex, the monsoon trough and the western disturbances. For example, types 7, 9, 12 and 18 are dominating patterns during wintertime accompanied by the polar vortex entering into Siberia. Types 8, 15, 16 and 17, which have a very broad and deep East Asia trough around the east coast of the Eurasian continental mainly appear during December to March. A continental high, the Iran High, is displayed in types 1, 3, 4, 11 and 14, mainly representing CTs of the wet season (May–September). However, an oceanic high, the western Pacific subtropical high is not very obvious in contour maps. Only types 2, 5, 6, 7 and 10 show faint signs in low latitudes during April, May, October and November. With corresponding anomaly patterns (filled contour plots in Figure 5), however, the western Pacific high can be identified in types 3, 4 and 11 north into southeastern China. Transient wave train can also be identified by the waves in the Ural Mountains (at the top left corner) and Kazakhstan.

TABLE 3 Circulation-type classifications of SAN ranked (lowest to highest) according to their performance (best to worst) when applied to the daily mean temperature and precipitation for the dry season (October–April) and wet season (May–September). The top one third of CTCs are marked in bold, and the bottom one third of CTCs are marked in italics

CTCs series	Temperature				Precipitation grade			
	Dry season		Wet season		Dry season		Wet season	
	EV	KS	EV	KS	EV	KS	EV	KS
Domain 1_09	7	3	4	2	<i>10</i>	2	<i>10</i>	2
Domain 1_18	3	<i>12</i>	2	9	<i>8</i>	4	<i>5</i>	5
Domain 1_27	1	<i>11</i>	1	3	<i>5</i>	<i>12</i>	3	<i>12</i>
Domain 2_09	<i>10</i>	2	7	1	<i>6</i>	1	<i>8</i>	1
Domain 2_18	4	9	5	5	4	6	6	3
Domain 2_27	2	<i>10</i>	3	<i>10</i>	1	<i>10</i>	2	9
Domain 3_09	<i>11</i>	4	<i>11</i>	4	<i>11</i>	3	<i>11</i>	8
Domain 3_18	8	6	8	7	<i>9</i>	5	<i>7</i>	4
Domain 3_27	5	7	6	8	3	<i>11</i>	1	<i>10</i>
Domain 4_09	<i>12</i>	1	<i>12</i>	6	<i>12</i>	8	<i>12</i>	6
Domain 4_18	9	5	<i>10</i>	<i>11</i>	<i>7</i>	7	8	7
Domain 4_27	6	8	9	<i>12</i>	2	9	4	<i>11</i>

5 | EVALUATION OF CIRCULATION-TYPE CLASSIFICATIONS FOR RESOLVING SPATIOTEMPORAL CLIMATE VARIATIONS

To do more comprehensively investigation about the suitability of CTCs for synoptic-climatological analyses in the CETP, the ability of CTCs to describe the spatiotemporal

variations of the surface climate variables was evaluated. Scatter diagrams plotted using the z -scores (i.e., subtracting the overall mean from each value and dividing by the standard deviation) of the EV and KS as coordinates were used to reveal their spatial descriptive ability of the targeted climate variables under synoptic-scale variations. The scatter diagrams consist of four quadrants. Each point on a given diagram represents a meteorological station. These stations were marked with different symbols on the maps in the right column of Figures 6 and 7 to denote the quadrant to which they belong. Quadrants represent the descriptive ability of the CTCs for climate variables. Stations in which climate variable variations were best resolved by the CTCs are located in the northeast quadrant (quadrant 1), and worst ones are located in the southwest quadrant (quadrant 3). Based on the results of section 4, two CTCs stand out: KRZ-CTC and SAN-CTC with the configuration of domain 2 and 18 CTs. They will be subject to further analysis.

Figures 6 and 7 show seasonal scatter plots and the corresponding maps obtained from the SAN-CTC series application on the daily mean temperature and precipitation grade, respectively. The superior CTCs (SAN-CTC and KRZ-CTC) obtained in section 4 were broadly similar in their performance in resolving the spatiotemporal variation of the daily mean temperature and precipitation. Both CTCs performed best in conditioning daily mean temperature variations in the Qaidam Basin and Qilian Mountains

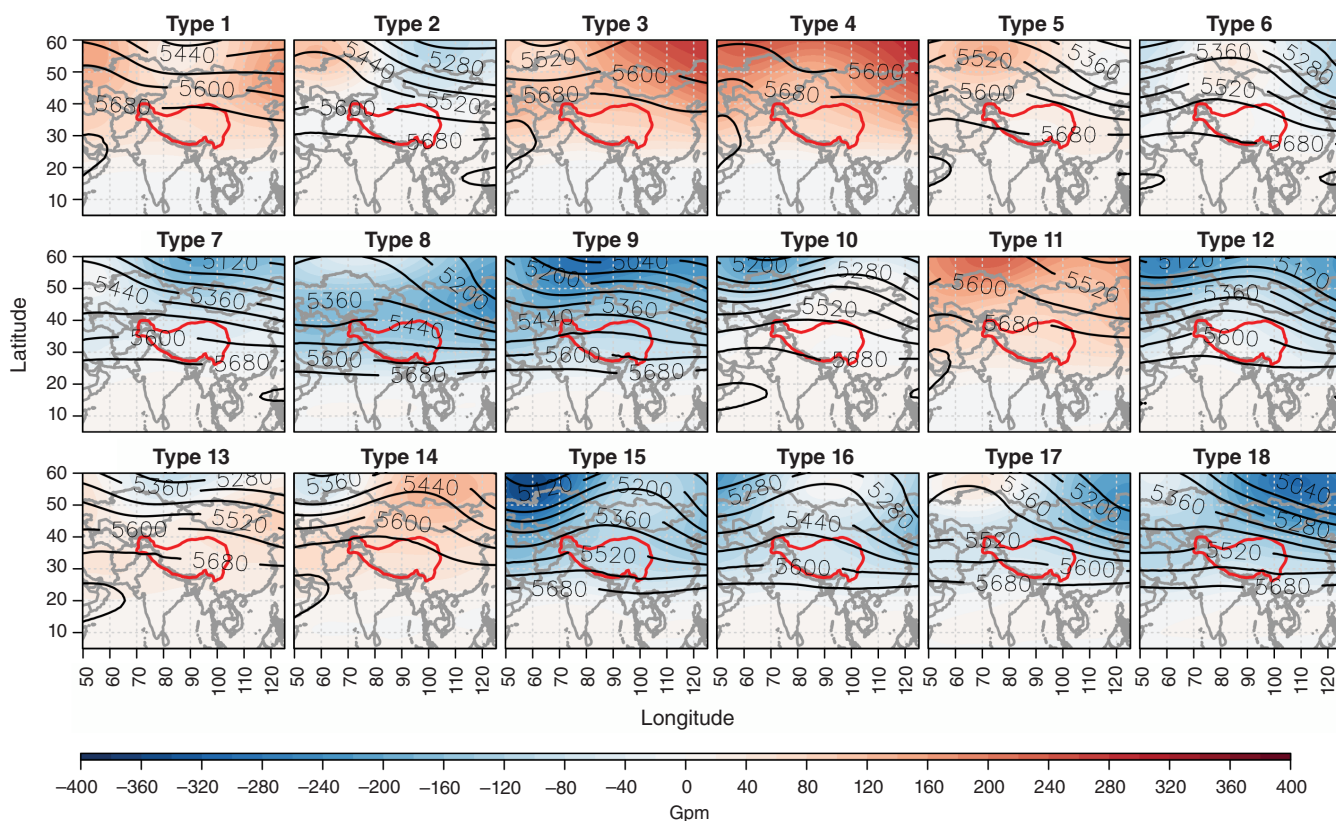


FIGURE 5 Typical SAN CTs of 500 hPa geopotential height for the period 1980–2014. The filled colour indicates their corresponding anomaly patterns [Colour figure can be viewed at wileyonlinelibrary.com]

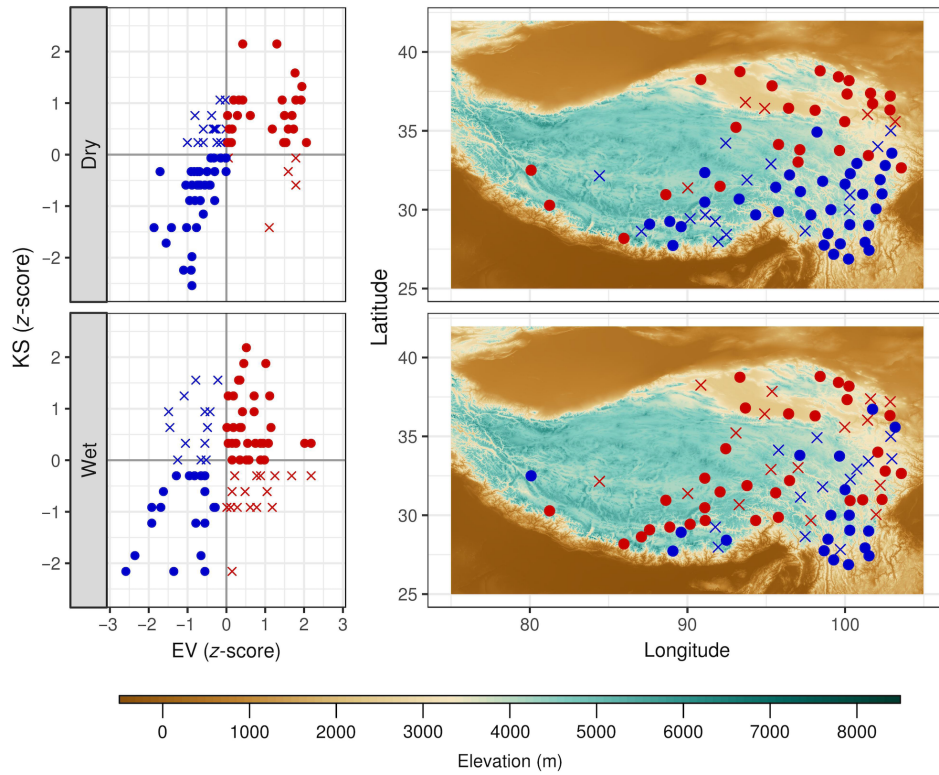


FIGURE 6 Seasonal scatter diagrams (left column) represent the ability of SAN-CTC to describe the temporal variation of daily mean temperature in each station. The abscissa denotes the relationship between daily mean temperature and SAN-CTC, the ordinate stands for the separability of daily mean temperature variations based on the CTCs series. The performance of the 80 stations is projected in to maps (the right column) to illustrate the spatial characters of SAN-CTC on resolving daily mean temperature variations [Colour figure can be viewed at wileyonlinelibrary.com]

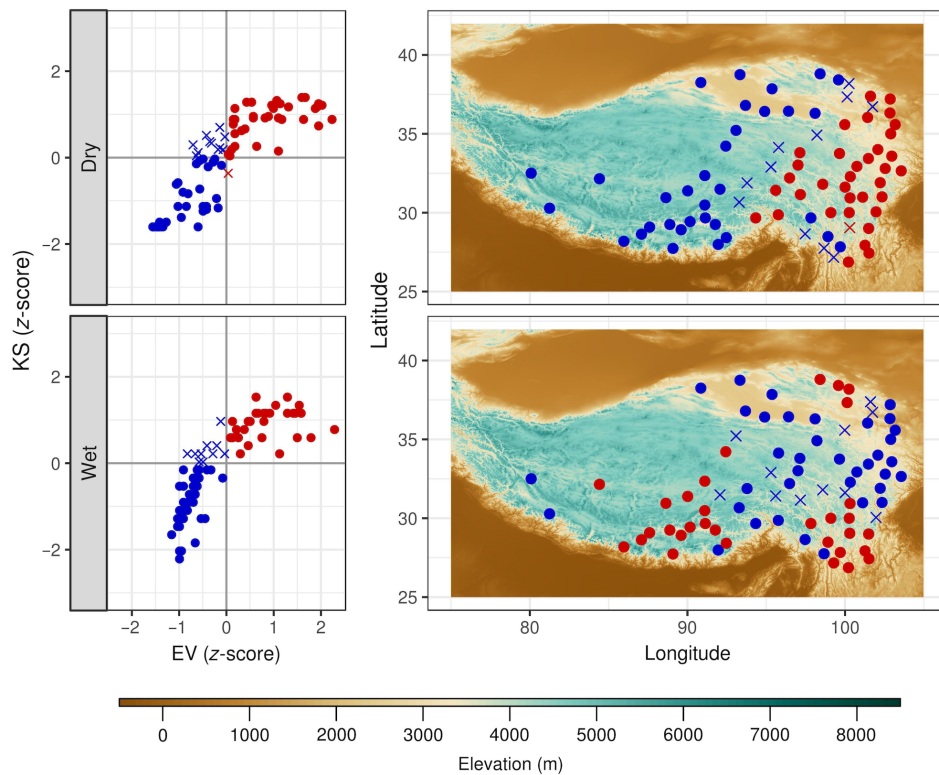


FIGURE 7 Seasonal scatter diagrams (left column) represent the ability of SAN-CTC to describe the temporal variation of precipitation grade in each station. The abscissa denotes the relationship between precipitation grade and SAN-CTC, the ordinate stands for the separability of precipitation grade variations based on the CTCs series. The performance of the 80 stations is projected in to maps (the right column) to illustrate the spatial characters of SAN-CTC on resolving precipitation grade variations [Colour figure can be viewed at wileyonlinelibrary.com]

(90°–103°E and 35°–40°N). In the wet season, the additional area between the Tanggula Mountains and the Himalayan Mountains (88°–97°E and 30°–34°N) presented a closer relationship with the CTCs than the steep slope area. With respect to the EV of the grouped daily mean temperature in well-conditioned regions, we found that 17.5–25.2% of the temperature variance in the dry season and 11.1–16.1% in the wet season were captured by the CTCs, which was much lower than the year-round situation, which ranged from 43.9 to 62.4%. For precipitation, the difference was rather small because the CTCs could only explain a small part of the synoptic-scale precipitation variation, even at the annual scale (less than 40% of the EV). Although the EV was low, spatial variations were well captured by the CTCs at the seasonal scale. In the dry season, large-scale circulations showed a closer relationship with daily precipitation variations in the eastern TP. However, in the wet season, higher CTC explanatory power was observed in the region ranging from the Brahmaputra River Basin to the Tanggula Mountains (85°–92°E and 28°–32°N) and the southern Hengduan Mountains (98°–102°E and 27°–31°N).

6 | DISCUSSION AND CONCLUSIONS

This work presented an investigation of the applicability of six CCMs according to a synoptic-climatological analysis in the CETP. The effects of different configurations in terms of the domain size and the numbers of CTs were examined. To compare and evaluate the CCMs, two statistical measures were used to quantify the within-group similarity and between-group separability among the CTC-grouped climate data.

Consistent with previous studies (Cahynová and Huth, 2016; Casado and Pastor, 2016; Huth *et al.*, 2016), there is no single most suitable CCM that could link the atmospheric circulation with the two surface climate variables. However, the EV and KS indicate that the optimization methods (SAN and SOM) and KRZ performed relatively well in the CETP. In KRZ, only the first three components are retained and all CTs are derived from their different combinations based on principal components and their corresponding amplitudes (Kruizinga, 1979; Buishand and Brandsma, 1997). The first three principal components can explain 73–86% variance of circulation variations. With the purpose of investigating main circulation characters and relationship between circulation and climate element variations in the TP, the first three principal components are considered to be able to offer most of the valuable information. Therefore, taking account of the amplitude of the first three components is more valuable than considering the remaining principal components. This makes KRZ more suitable than any other principal component analysis based CCMs. The optimization CCMs are actually pure mathematical approaches. They adopt discriminant function to do a similarity judgement and iteration

adaptation procedure to obtain optimal classification results. The two optimal methods identified show almost identical results in all configurations. However, in the implementations, SAN just needs to update one cluster centroid while SOM requires update weights of the winning neuron and its neighbours. This makes SAN more computationally efficient than SOM and slightly better in terms of classification accuracy. Taken together, KRZ and SAN are recommended for classifying the atmospheric circulation over the TP.

The ability to resolve synoptic-scale climate variations presented limited improvements via the inclusion of CTCs with 27 CTs relative to those with 18 CTs. This finding suggests that CTCs with 27 CTs are over-refined, which was further proven in the ranking of CTCs with different configurations, where the CTCs obtained in domain 2 with 18 CTs presented a slight advantage.

Using the *z*-score of the EV and KS scores, a suitability evaluation of CTCs in the CETP was conducted by investigating the resolving power for captured spatiotemporal climate variation at the seasonal scale. Two selected CTCs (SAN-CTC and KRZ-CTC in domain 2 with 18 CTs) present a similar ability in representing spatiotemporal variations. The results demonstrate that large-scale CTCs are better at capturing the seasonal variation than intra-seasonal variations as they could capture 43.9–62.4% of the temperature variance all year round. At the seasonal scale, the EV decreased to 17.5–25.2% in the dry season and 11.1–16.1% in the wet season. The results of this study can be compared with those of previous studies in Europe. For example, Broderick and Fealy (2015) found that CTCs generally performed best for winter in Ireland, which reflected the close coupling between circulation and surface conditions. Cahynova and Huth (2010) found that seasonal temperature and precipitation trends could only be partly explained by the changing frequency of CTs and that the link was strongest in winter.

We suggest that the differences between our study and previous studies be explained by two reasons. One reason is the division of the seasons because the dry season in this study included the entire winter as well as most of spring and autumn. The other reason is due to the fact that large-scale controls on surface–atmosphere interaction were exerted by the elevation of the land surface and the orientation and extent of the TP, which led to typical seasonal circulation patterns, namely, the westerly circulation and the monsoon circulation. These controls can be illustrated by the linking CTCs with spatiotemporal variations of climate variables. In the dry season, CTCs performed well for daily mean temperature variations recorded at stations in the northeastern TP, including the Qaidam Basin and the Qilian Mountains (90°–103°E and 35°–40°N), compared with that of the other stations. In the wet season, the daily mean temperature variations recorded at stations in the northeastern TP and the area between the Tanggula Mountains and the

Himalayan Mountains (88°–97°E and 30°–34°N) also had a closer relationship with the CTCs than other stations in steep slope areas.

The CTCs used in this study were obtained from 500 hPa geopotential height data, and this level belongs to the free atmosphere in the northeastern TP. Therefore, advections in this region can be well described by CTCs. In the southern region, we inferred that the better performance of the CTCs in stratifying the daily mean temperature variations was related to water vapour transport. Yanai and Li (1994) found that the sensible heat flux from the surface before the onset of summer rains is the major source of heating on the TP. After the onset of summer rains, the heat released by condensation is the primary source of heating over the TP.

According to the EV of the CTC-grouped precipitation grade, the CTCs performed poorly in resolving the CETP precipitation variation. This poor performance may have been caused by the nature of the precipitation data. Daily precipitation has a discrete-continuous character that consists of the occurrence and intensity of a given event. Large-scale circulation mainly represents possible vapour channels and has a close relationship with precipitable water. However, the occurrence of precipitation is also affected by factors other than large-scale circulation such as topography. Therefore, CTCs have a better ability in resolving precipitation at monthly or seasonal scales (e.g., Liu *et al.*, 2015) than at daily scale. Although relatively low EV was observed, the spatiotemporal variation obtained from the CTCs could reflect some dominant climatological processes. In the dry season, large-scale circulations show a closer relationship with daily precipitation variations in the eastern TP because less precipitation occurred during that period and precipitation was mainly caused by the combined effect of warm and moisture-laden flow east to the southwesterly trough and cold air from Siberia in that area. In the wet season, CTCs had a fair performance in the region ranging from the Brahmaputra River basin to the Tanggula Mountains and the southern Hengduan Mountains. Corresponding to these two regions are two major water vapour paths and affect zone that transport water vapour from the Indian Ocean and the Bay of Bengal into the TP via the western boundary and the southern boundary of the TP (Zhang *et al.*, 2017).

In general, CTCs performed well in resolving the seasonal variations of daily mean temperature but performed poorly in resolving the intra-seasonal variations of daily precipitation and daily mean temperature. Two superior CTCs, SAN-CTC and KRZ-CTC, in domain 2 with 18 CTs exhibited similar performance in revealing the spatiotemporal variation of the two climate variables. The daily mean temperature variations recorded at the stations in the northeastern TP, that is, the region of the Qaidam Basin and the Qilian Mountains, were well resolved by the CTCs for both seasons compared with the variations at the other stations.

Additionally, the daily mean temperature variations in the wet season in the area between the Tanggula Mountains and the Himalayan Mountains had a closer relationship with the CTCs than with stations in the steeper slope areas.

Although the CTC series were not well related to the time series of precipitation grade of stations in the CETP, they could reflect certain climatological processes observed in the spatiotemporal variations of daily precipitation. In the dry season, large-scale circulations indicated a closer relationship with daily precipitation variation in the eastern TP. However, in the wet season, higher explanatory power was shown in a region of the Brahmaputra River basin to the Tanggula Mountains (85°–92°E and 28°–32°N) and the southern Hengduan Mountains (98°–102°E and 27°–31°N).

ACKNOWLEDGEMENTS

We thank the two anonymous reviewers whose comments and suggestions helped improve and clarify this paper. This research was supported by the National Natural Science Foundation of China (Grant No. 91537210), the Strategic Priority Research Program of Chinese Academy of Sciences (XDA20060401), Swedish VR, VINOVA, STINT, BECC, MERGE and SNIC through S-CMIP.

ORCID

Xiaowen Zhang  <http://orcid.org/0000-0002-2898-342X>

Deliang Chen  <http://orcid.org/0000-0003-0288-5618>

REFERENCES

- Ahasan, M.N., Chowdhury, M.A.M. and Quadir, D.A. (2014) The summer monsoon weather systems and its relationship with rainfall over South Asia. *Open Journal Atmospheric Climate Change*, 1(2), 2374–3808.
- Baur, F., Hess, P. and Nagel, H. (1944) *Kalender der Grosswetterlagen Europas 1881–1939*. Germany: Bad Homburg.
- Beck, C. and Philipp, A. (2010) Evaluation and comparison of circulation type classifications for the European domain. *Physics and Chemistry of the Earth*, 35(9–12), 374–387. <https://doi.org/10.1016/j.pce.2010.01.001>.
- Beck, C., Jacobeit, J. and Jones, P.D. (2007) Frequency and within-type variations of large-scale circulation types and their effects on low-frequency climate variability in central Europe since 1780. *International Journal of Climatology*, 27(4), 473–491. <https://doi.org/10.1002/joc.1410>.
- Broderick, C. and Fealy, R. (2015) An analysis of the synoptic and climatological applicability of circulation type classifications for Ireland. *International Journal of Climatology*, 35(4), 481–505. <https://doi.org/10.1002/joc.3996>.
- Buishand, T.A. and Brandsma, T. (1997) Comparison of circulation classification schemes for predicting temperature and precipitation in the Netherlands. *International Journal of Climatology*, 17(8), 875–889. [https://doi.org/10.1002/\(SICI\)1097-0088\(19970630\)17:8<875::AID-JOC164>3.0.CO;2-C](https://doi.org/10.1002/(SICI)1097-0088(19970630)17:8<875::AID-JOC164>3.0.CO;2-C).
- Cahynova, M. and Huth, R. (2010) Circulation vs. climatic changes over the Czech Republic: a comprehensive study based on the COST733 database of atmospheric circulation classifications. *Physics and Chemistry of the Earth*, 35(9–12), 422–428. <https://doi.org/10.1016/j.pce.2009.11.002>.
- Cahynová, M. and Huth, R. (2016) Atmospheric circulation influence on climatic trends in Europe: an analysis of circulation type classifications from the COST733 catalogue. *International Journal of Climatology*, 36(7), 2743–2760. <https://doi.org/10.1002/joc.4003>.
- Casado, M.J. and Pastor, M.A. (2016) Circulation types and winter precipitation in Spain. *International Journal of Climatology*, 36(7), 2727–2742. <https://doi.org/10.1002/joc.3860>.

- Casado, M.J., Pastor, M.A. and Doblas-Reyes, F.J. (2010) Links between circulation types and precipitation over Spain. *Physics and Chemistry of the Earth, Parts A/B/C*, 35(9–12), 437–447. <https://doi.org/10.1016/j.pce.2009.12.007>.
- Cavazos, T. (1999) Large-scale circulation anomalies conducive to extreme precipitation events and derivation of daily rainfall in northeastern Mexico and southeastern Texas. *Journal of Climate*, 12(5), 1506–1523. [https://doi.org/10.1175/1520-0442\(1999\)012<1506:LSCACT>2.0.CO;2](https://doi.org/10.1175/1520-0442(1999)012<1506:LSCACT>2.0.CO;2).
- Chen, D. (2000) A monthly circulation climatology for Sweden and its application to a winter temperature case study. *International Journal of Climatology*, 20(10), 1067–1076. [https://doi.org/10.1002/1097-0088\(200008\)20:10<1067::AID-JOC528>3.0.CO;2-Q](https://doi.org/10.1002/1097-0088(200008)20:10<1067::AID-JOC528>3.0.CO;2-Q).
- Chen, D., Xu, B., Yao, T., Guo, Z., Cui, P., Chen, F., Zhang, R., Zhang, X., Zhang, Y., Fan, J., Hou, Z. and Zhang, T. (2015) Assessment of past, present and future environmental changes on the Tibetan Plateau. *Chinese Science Bulletin*, 60: 3025–3035. <https://doi.org/10.1360/N972014-01370>. (in Chinese with English abstract)
- Corte-Real, J., Qian, B. and Xu, H. (1998) Regional climate change in Portugal: precipitation variability associated with large-scale atmospheric circulation. *International Journal of Climatology*, 18(6), 619–635. [https://doi.org/10.1002/\(SICI\)1097-0088\(199805\)18:6<619::AID-JOC271>3.0.CO;2-T](https://doi.org/10.1002/(SICI)1097-0088(199805)18:6<619::AID-JOC271>3.0.CO;2-T).
- Dee, D.P., Uppala, S.M., Simmons, A.J., Berrisford, P., Poli, P., Kobayashi, S., Andrae, U., Balmaseda, M.A., Balsamo, G., Bauer, P., Bechtold, P., Beljaars, A.C.M., van de Berg, L., Bidlot, J., Bormann, N., Delsol, C., Dragani, R., Fuentes, M., Geer, A.J., Haimberger, L., Healy, S.B., Hersbach, H., Hólm, E.V., Isaksen, I., Kållberg, P., Köhler, M., Matricardi, M., McNally, A.P., Monge-Sanz, B.M., Morcrette, J.-J., Park, B.-K., Peubey, C., de Rosnay, P., Tavolato, C., Thépaut, J.-N. and Vitart, F. (2011) The ERA-Interim reanalysis: configuration and performance of the data assimilation system. *Quarterly Journal of the Royal Meteorological Society*, 137(656), 553–597. <https://doi.org/10.1002/qj.828>.
- Fettweis, X., Mabilille, G., Erpicum, M., Nicolay, S. and den Broeke, M.V. (2010) The 1958–2009 Greenland ice sheet surface melt and the mid-tropospheric atmospheric circulation. *Climate Dynamics*, 36(1–2), 139–159. <https://doi.org/10.1007/s00382-010-0772-8>.
- Gao, Y., Cuo, L. and Zhang, Y. (2014) Changes in moisture flux over the Tibetan Plateau during 1979–2011 and possible mechanisms. *Journal of Climate*, 27, 1876–1893. <https://doi.org/10.1175/JCLI-D-13-00321.1>.
- Gevorgyan, A. (2013) Main types of synoptic processes and circulation types generating heavy precipitation events in Armenia. *Meteorology and Atmospheric Physics*, 122(1–2), 91–102. <https://doi.org/10.1007/s00703-013-0270-8>.
- Hess, P. and Brezowsky, H. (1952) *Katalog Der Großwetterlagen Europas Ber. Dt. Wetterd.* US-Zone 33/US-Zone 33.
- Huth, R. (2000) A circulation classification scheme applicable in GCM studies. *Theoretical and Applied Climatology*, 67(1–2), 1–18. <https://doi.org/10.1007/s007040070012>.
- Huth, R. (2010) Synoptic-climatological applicability of circulation classifications from the COST733 collection: first results. *Physics and Chemistry of the Earth, Parts A/B/C*, 35(9–12), 388–394. <https://doi.org/10.1016/j.pce.2009.11.013>.
- Huth, R., Beck, C., Philipp, A., Demuzere, M., Ustrnul, Z., Cahynová, M., Kyselý, J. and Tveit, O.E. (2008) Classifications of atmospheric circulation patterns. *Annals of the New York Academy of Sciences*, 1146(1), 105–152. <https://doi.org/10.1196/annals.1446.019>.
- Huth, R., Beck, C. and Kučerová, M. (2016) Synoptic-climatological evaluation of the classifications of atmospheric circulation patterns over Europe. *International Journal of Climatology*, 36(7), 2710–2726. <https://doi.org/10.1002/joc.4546>.
- James, P.M. (2006) An objective classification method for Hess and Brezowsky Grosswetterlagen over Europe. *Theoretical and Applied Climatology*, 88(1–2), 17–42. <https://doi.org/10.1007/s00704-006-0239-3>.
- Jenkinson, A. and Collinson, F. (1977) An initial climatology of gales over the North Sea. *Synoptic Climatology Branch Memorandum*, 62, 18.
- Jones, G.V. and Davis, R.E. (2000) Using a synoptic climatological approach to understand climate–viticulture relationships. *International Journal of Climatology*, 20(8), 813–837. [https://doi.org/10.1002/1097-0088\(200006\)20:8<813::AID-JOC495>3.0.CO;2-W](https://doi.org/10.1002/1097-0088(200006)20:8<813::AID-JOC495>3.0.CO;2-W).
- Kirchhofer, W. (1974) Classification of European 500 Mb Patterns, Schweiz. Meteorol. Anstalt, Inst. Suisse Meteorol., Zurich, 43, 1–16.
- Kohonen, T. (1990) The self-organizing map. *Proceedings of the IEEE*, 78(9), 1464–1480. <https://doi.org/10.1109/5.58325>.
- Kruizinga, S. (1979) Objective classification of daily 500 mbar patterns. Preprints Sixth Conference on Probability and Statistics in the Atmospheric Sciences, 9–12. October, Banff, Alberta. American Meteorological Society: Boston, MA; 126–129.
- Kyselý, J. (2002) Temporal fluctuations in heat waves at Prague-Klementinum, The Czech Republic, from 1901–97, and their relationships to atmospheric circulation. *International Journal of Climatology*, 22(1), 33–50. <https://doi.org/10.1002/joc.720>.
- Lamb, H.H. (1950) Types and spells of weather around the year in the British Isles: annual trends, seasonal structure of the year, singularities. *Quarterly Journal of the Royal Meteorological Society*, 76(330), 393–429. <https://doi.org/10.1002/qj.49707633005>.
- Lamb, H.H. (1972) *British Isles weather types and a register of daily sequence of circulation patterns 1861–1971*. London: H.M. Stationery Office.
- Liu, X. and Chen, B. (2000) Climatic warming in the Tibetan Plateau during recent decades. *International Journal of Climatology*, 20(14), 1729–1742. [https://doi.org/10.1002/1097-0088\(20001130\)20:14<1729::AID-JOC556>3.0.CO;2-Y](https://doi.org/10.1002/1097-0088(20001130)20:14<1729::AID-JOC556>3.0.CO;2-Y).
- Liu, W., Wang, L., Chen, D., Tu, K., Ruan, C. and Hu, Z. (2015) Large-scale circulation classification and its links to observed precipitation in the eastern and central Tibetan Plateau. *Climate Dynamics*, 1–17. <https://doi.org/10.1007/s00382-015-2782-z>.
- Michaelides, S.C., Liassidou, F. and Schizas, C.N. (2007) Synoptic classification and establishment of analogues with artificial neural networks. *Pure and Applied Geophysics*, 164(6–7), 1347–1364. <https://doi.org/10.1007/s00024-007-0222-7>.
- Philipp, A., Della-Marta, P.M., Jacobeit, J., Fereday, D.R., Jones, P.D., Moberg, A. and Wanner, H. (2007) Long-term variability of daily North Atlantic–European pressure patterns since 1850 classified by simulated annealing clustering. *Journal of Climate*, 20(16), 4065–4095. <https://doi.org/10.1175/JCLI4175.1>.
- Philipp, A., Beck, C., Esteban, P., Kreienkamp, F., Krennert, T., Lochbihler, K., Lykoudis, S.P., Pianko-Kluczynska, K., Post, P., Alvarez, D.R., Spekat, A. and Streicher, F. (2014) *cost733class-1.2 user guide*.
- Philipp, A., Beck, C., Huth, R. and Jacobeit, J. (2016) Development and comparison of circulation type classifications using the COST 733 dataset and software. *International Journal of Climatology*, 36(7), 2673–2691. <https://doi.org/10.1002/joc.3920>.
- Plaut, G. and Simonnet, E. (2001) Large-scale circulation classification, weather regimes, and local climate over France, the Alps and western Europe. *Climate Research*, 17(3), 303–324. <https://doi.org/10.3354/cr017303>.
- Richman, M.B. (1986) Rotation of principal components. *Journal of Climatology*, 6(3), 293–335. <https://doi.org/10.1002/joc.3370060305>.
- Schiemann, R. and Frei, C. (2010) How to quantify the resolution of surface climate by circulation types: an example for alpine precipitation. *Physics and Chemistry of the Earth, Parts A/B/C*, 35(9–12), 403–410. <https://doi.org/10.1016/j.pce.2009.09.005>.
- Schmutz, C. and Wanner, H. (1998) Low frequency variability of atmospheric circulation over Europe between 1785 and 1994 (Niederfrequente Schwankungen der atmosphärischen Zirkulation über Europa zwischen 1785 und 1994). *Erdkunde*, 52, 81–94.
- Tveit, O.E. (2010) An assessment of circulation type classifications for precipitation distribution in Norway. *Physics and Chemistry of the Earth, Parts A/B/C*, 35(9–12), 395–402. <https://doi.org/10.1016/j.pce.2010.03.044>.
- Wu, G., Duan, A., Liu, Y., Mao, J., Ren, R., Bao, Q., He, B., Liu, B. and Hu, W. (2015) Tibetan Plateau climate dynamics: recent research progress and outlook. *National Science Review*, 2(1), 100–116. <https://doi.org/10.1093/nsr/nwu045>.
- Yanai, M. and Li, C. (1994) Mechanism of heating and the boundary layer over the Tibetan Plateau. *Monthly Weather Review*, 122(2), 305–323. [https://doi.org/10.1175/1520-0493\(1994\)122<0305:MOHATB>2.0.CO;2](https://doi.org/10.1175/1520-0493(1994)122<0305:MOHATB>2.0.CO;2).
- Yao, T., Masson-Delmotte, V., Gao, J., Yu, W., Yang, X., Risi, C., Sturm, C., Werner, M., Zhao, H. and He, Y. (2013) A review of climatic controls on $\delta_{18}O$ in precipitation over the Tibetan Plateau: observations and simulations. *Reviews of Geophysics*, 51(4), 525–548. <https://doi.org/10.1002/rog.20023>.
- Yarnal, B. (1993) *Synoptic Climatology in Environmental Analysis*. London: Belhaven Press.

- Yarnal, B., Comrie, A.C., Frakes, B. and Brown, D.P. (2001) Developments and prospects in synoptic climatology. *International Journal of Climatology*, 21(15), 1923–1950. <https://doi.org/10.1002/joc.675>.
- Ye, D. and Gao, Y. (1979) *Meteorology of Qinghai-Xizang (Tibet) Plateau*. Beijing: Science Press. (in Chinese).
- Ye, D. and Wu, G. (1998) The role of the heat source of the Tibetan Plateau in the general circulation. *Meteorology and Atmospheric Physics*, 67(1–4), 181–198. <https://doi.org/10.1007/BF01277509>.
- Zhang, C., Tang, Q. and Chen, D. (2017) Recent changes in the moisture source of precipitation over the Tibetan Plateau. *Journal of Climate*, 30(5), 1807–1819. <https://doi.org/10.1175/JCLI-D-15-0842.1>.
- Zhu, Y., Chen, D., Li, W. and Zhang, P. (2007) Lamb–Jenkinson circulation type classification system and its application in China. *Journal of Nanjing Institute of Meteorology*, 30(3), 289–297 (in Chinese with English abstract).

SUPPORTING INFORMATION

Additional supporting information may be found online in the Supporting Information section at the end of the article.

How to cite this article: Zhang X, Chen D, Yao T. Evaluation of circulation-type classifications with respect to temperature and precipitation variations in the central and eastern Tibetan Plateau. *Int J Climatol*. 2018;38:4938–4949. <https://doi.org/10.1002/joc.5708>